

Development of Ultra High Strength Mn-B Steels for Automobile Door Impact Tube

JUI-FAN TU*, YEONG-TSUEN PAN*, CHING-YUAN HUANG* and SHEAU-HWA HSIEH**

*Steel and Aluminum Research and Development Department

**New Materials Research and Development Department

China Steel Corporation

The mechanical properties and delayed fracture resistance of quenched ultra high strength MnB steel were investigated in this study. The MnB steel exhibited tensile strength up to 1600MPa~1760MPa and kept a good ductility through various induction heating processes followed by a sprayed water quenching. The corresponding microstructure is composed of a fully martensitic structure without retained or tempered carbides. An extremely fine prior austenite grain size ranging from 2.5 to 8 μ m was obtained from the fast induction heating process. The delayed fracture test showed that the quenched MnB steel possessed a good delayed fracture resistance in a dilute acid solution. The critical hydrogen content of the quenched MnB steel for the occurrence of delayed fracture, determined by the electrochemical hydrogen charged specimens under the constant load test of yield stress, is 3.7ppm.

1. INTRODUCTION

Figure 1 shows the prerequisite automobile door impact beam (DIB) of modern sedans, which acts as one of the safety parts to reduce the direct side impact threat to passengers and to enhance the anti distortion locking of a car door suffering a side impact. For weight-saving and strengthening concerns, the heat treated tubular DIB has been gradually substituted for the conventional cold stamped channel in the development of modern automobiles.

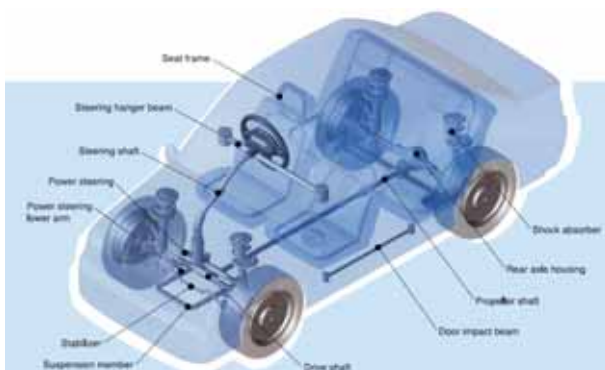


Fig. 1. Door impact beam in an automobile.

According to the specification of No. 214 of FMVSS (Federal Motor Vehicle Safety Standard), America, most automobile manufacturers specify the properties requirement for automobile DIB as: tensile strength higher than 1,100MPa; yield strength higher than 800 MPa; and total elongation longer than 10%. Low carbon MnB steel featuring excellent quench hardenability can achieve the required properties of DIB.^(1,2)

Tubular DIB can be produced by using the Electric Resistance Welded (ERW) process⁽³⁾, as shown in Figure 2. The slit steel plate is first rolled to a tubular shape through a series of forming and fine rolls, and then is welded via an induction heating coil and a pair of welded rolls. A DIB tube is generally hardened through a high frequency induction heat treatment, which features quickness, cleanness, high efficiency, ease to automatization and in-line production, and is an environmentally friendly heating technology. In addition, the application of high pressure water spray significantly increases the quenching rate of steel, resulting in a higher hardness and strength than conventionally quenched steel and thus achieving weight-saving. The principle of induction heating is to obtain the heat through an induced eddy current. The heating depth of induction heating and the working frequency keep the following relationship⁽⁴⁾ expressed as equation (1):

$$\delta(cm) = \frac{1}{2\pi} \sqrt{\frac{\rho}{\mu f}} \dots\dots\dots (1)$$

Where ρ = resistivity (n Ω -cm) ; f = frequency (Hz) ;
and μ = permeability.

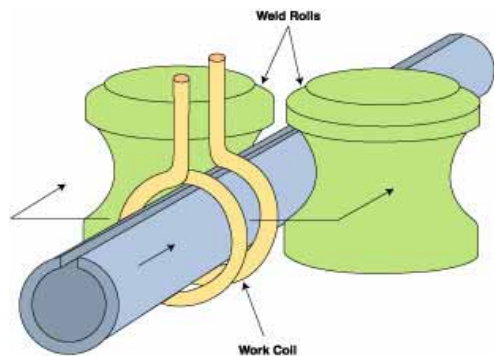


Fig. 2. Schematic illustration of ERW process for steel tubing.

It has been suggested that high strength steel where the yield strength is greater than 1,100MPa is highly sensitive to hydrogen embrittlement (HE). That is to say, the mechanical properties of DIB might deteriorate or even suffer rupture once the hydrogen is absorbed during steelmaking, rolling, heating treatment, pickling and plating or is exposed during application to a hydrogen-enriched environment. The literature⁽⁵⁾ points out that the hydrogen atoms in the steel can be categorized into two types as shown in Figure 3: (1) diffusible hydrogen atoms under 200 ; (2) non-diffusible hydrogen atoms. At room temperature, the diffusible hydrogen can easily diffuse into stress concentrated regions because the hydrogen trap sites feature a weak binding energy, such as dislocation, and can not trap the hydrogen causing HE. In contrast, the non- diffusible hydrogen trapped by the high binding energy trap sites at room temperature, such as retained austenite and semi-coherent interface, can not diffuse and will not result in HE⁽⁶⁾. Therefore, the increase of high binding energy trap sites to trap the penetrated hydrogen can enhance the delayed fracture resistance.

The purpose of this study is to investigate the effect of induction heating and quenching parameters on the mechanical properties, hardness, and delayed fracture resistance of MnB steel.

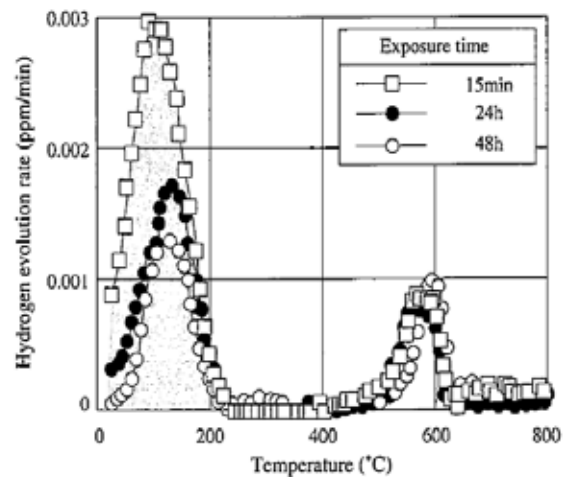


Fig. 3. Effect of exposure time in air at room temperature after hydrogen charge on hydrogen evolution curves as obtained by thermal analysis of hydrogen-charged specimens.

2. EXPERIMENTAL METHOD

The chemical composition of the 15B22 MnB steel is shown in Table 1. The hot rolled coil was slit and electric resistance welded into 31.8mm*2.0mm tubes. The steel tube was further induction heat treated by using various heating parameters to get a fully martensitic microstructure, as shown in Figure 4. Table 2 shows that these heating parameters include various quenching temperatures and heating rates with a given induction heating frequency of 300kHz. The as-heat treated tube was subjected to tensile and hardness testing to compare the effects of various induction heat treating conditions. Optical microscopy was used to measure the prior austenite grain size of as-heat treated specimens and to evaluate whether the martensite transformation was completed or not. The continuous cooling transformation diagram (CCT) of MnB steel was conducted by a dilatometer. The delayed fracture test was carried out for the specimens pre-immersed in a 5% hydrochloric acid solution then rapidly subjected to the constant loading of the yield strength based on the NSC’s test method. In addition, the specimens were also hydrogen charged, using electrochemical charging and nickel electroplating to preserve the charged hydrogen, in order to evaluate the maximum allowable hydrogen content. The hydrogen content was measured using a LECO DH603 hydrogen analyzer.

Table 1 Chemical composition of 15B22 steel in wt%

Alloy	C	Si	Mn	P	S	Ti	Cr	Al	B	Cu
15B22	0.22	0.2	1.15	0.014	0.008	0.02	0.22	0.043	0.0023	0.01

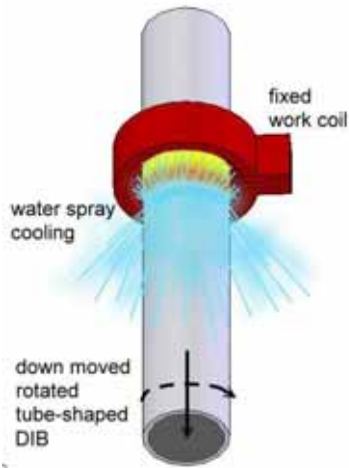


Fig. 4. Schematic illustration of induction heating and spray water quenching for tubular DIB.

Table 2 Various induction heating parameters at 300kHz

Quenching Temp.	Heating rate	
	400 /s	800 /s
850	A	E
900	B	F
950	C	G
1,000	D	H

3. RESULTS AND DISCUSSION

3.1 Microstructure and Mechanical Properties of Raw Tube

Figure 5 shows the microstructure of an as-received ERW 15B22 steel tube, which is composed of typical ferrite and pearlite. An around 20µm decarburization layer is observed in the as-received tube, which is considered to have originated from the hot rolling process. The properties of the as-received steel tube are: hardness~HRB 91-93, yield strength around 592MPa, tensile strength around 676MPa, and total elongation around 20%.

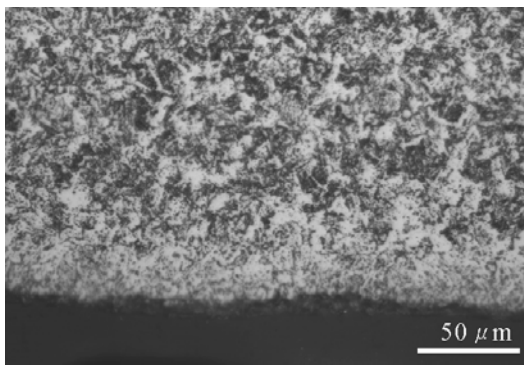


Fig. 5. Optical micrograph of as-received 15B22 steel tube.

3.2 CCT Diagram of 15B22 Steel

Figure 6 exhibits the CCT diagram of the 15B22 steel ($AC_3=823^\circ\text{C}$). The 15B22 steel with a good hardenability can be transformed into a fully martensitic structure when the cooling rate is greater than or equal to 30°C/s due to the effect of the boron and manganese additions. It should be noted that autotempering easily occurs in 15B22 steel because of its high M_s temperature, near to 400°C . However, as the average cooling rate of water spray cooling was consistently above 100°C/s , the 15B22 steel was transformed into the fully quenched martensite without problem.

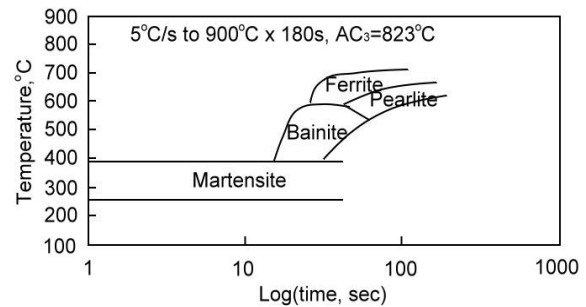


Fig. 6. CCT curve of 15B22.

3.3 Tensile Properties and Hardness of As-quenched Tube

Figure 7 shows the tensile properties of the as-quenched 15B22 steel tube ($\Phi 31.8\text{mm} \times 2.0\text{mm}$), indicating that the as-quenched steel tube can fully satisfy the minimum requirement for impact beam (YS 1180 MPa, TS 1470 MPa, total elongation 6%). Since the high frequency induction heating and quenching process features the merits of fast heating rate (400°C/s and 800°C/s) and rapid high pressure water cooling, the resulting martensite is extremely fine. Such a tube thus exhibits superior tensile properties compared with that treated by a conventional quenching process. It can be found the strength of the tube increases with an increasing quenching temperature and reaches a peak at 900°C . Such a phenomenon is more significant when a slow heating rate is applied. All the steel tubes exhibit total elongation longer than 12%, showing no specified trend with the increasing quenching temperature.

Figure 8 shows the hardness distribution of the 15B22 tubes in the cross section direction and indicates that the cross direction hardness can stably reach a level higher than HV 500 when the quenching temperature is higher than 900°C . It is noted that the hardness decreases with the depth from the surface when a quenching temperature of 850°C is applied, which becomes more pronounced when a higher heating rate is applied.

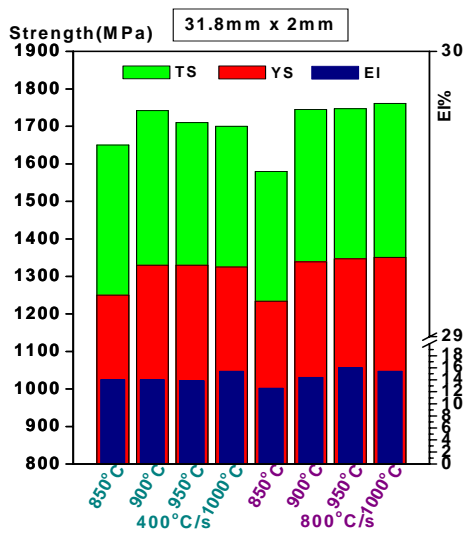


Fig. 7. Tensile properties of induction heated and quenched 15B22 at various induction heating conditions.

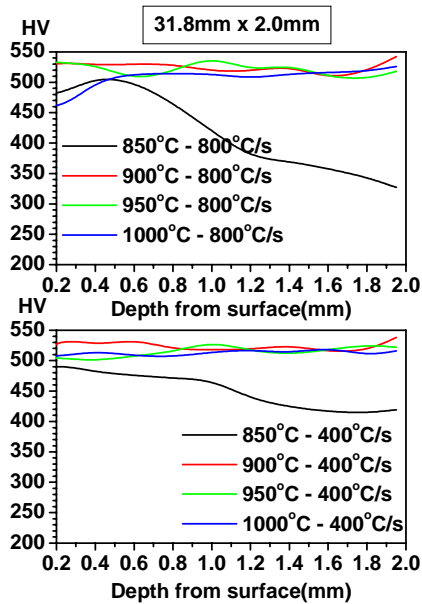


Fig. 8. The hardness distributions of various induction quenched 15B22 door impact beams in the cross section direction.

3.4 As-quenched Microstructure and Prior Austenite Grain Size

Figure 9 shows the TEM and OM microstructures of an as-quenched tube. It can be found that as-quenched 15B22 steel exhibits a typical low carbon lath martensite structure with abundant dislocation inside the martensite lath and is free of tempered carbides and residual carbides. According to the OM micrograph, the high frequency induction quenched martensite is extremely fine, thus resulting in an excellent combination of strength and elongation.

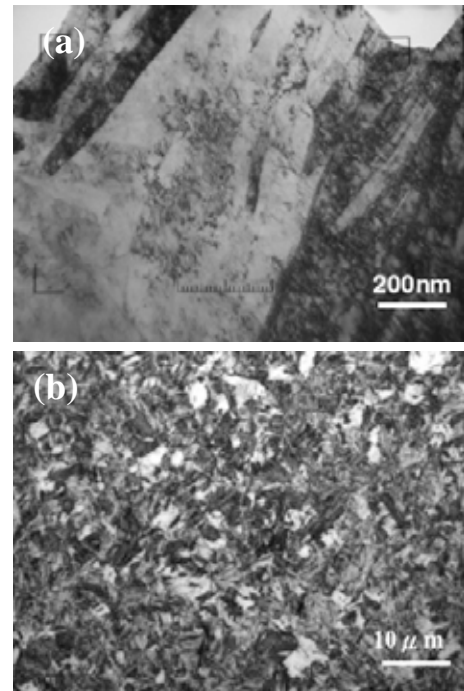


Fig. 9. Microstructures of induction quenched 15B22: (a)TEM, and (b)OM.

Figures 10 and 11 show the prior austenite grain size of an 15B22 steel tube subjected to various heat treating parameters. It can be found that the prior austenite grain size increases with increasing quenching temperature and decreasing heating rate. Note that the effect of quenching temperature is more remarkable than heating rate, which is contributed from the feature of a very high heating rate associated with the induction heating process. The resultant prior austenite grain size of induction heat treatment ranged from 2.5 to 8μm, which is smaller than that obtained using a convention furnace quenching process, thus offering an excellent combination of tensile properties (total elongation 12% and TS 1500MPa).

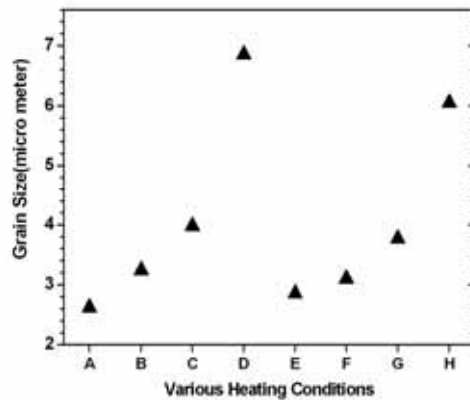


Fig. 10. Variation of prior austenite grain size of quenched 15B22 steel tubes on various induction heating conditions.

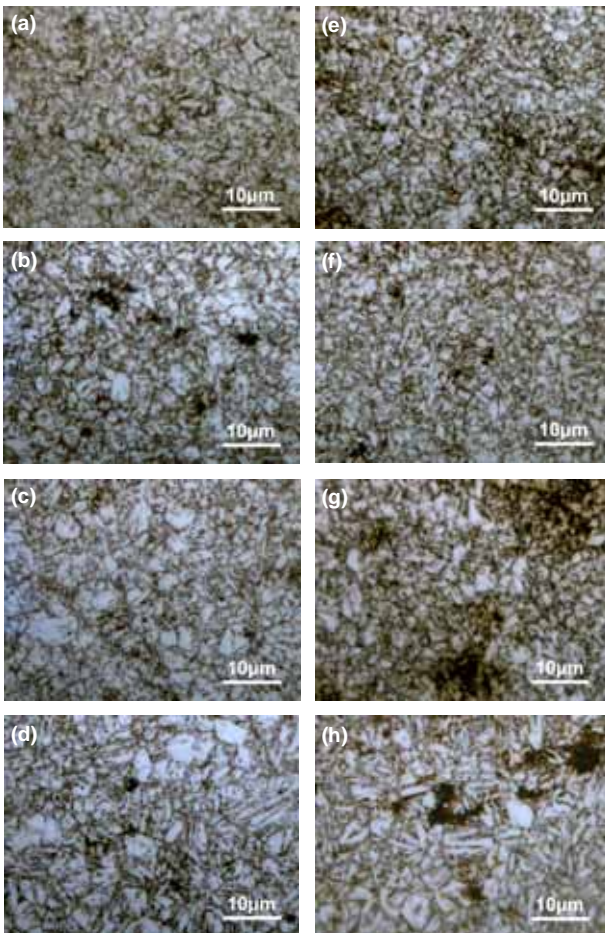


Fig. 11. Micrographs of prior austenite grain sizes of various condition quenched 15B22 steel tubes.

3.5 Observation of Fracture Surface

Figure 12 shows the typical tensile fractograph of an as-quenched 15B22 steel tube, indicating the ductile dimple features. Since the dimples are very fine and deep, it suggests that this MnB steel tube features high strength and excellent ductility as well as toughness.

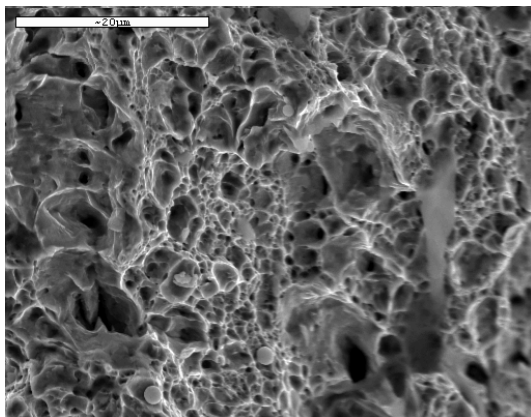


Fig. 12. Fracture morphology of 15B22 steel tube by induction quenching.

3.6 Delayed Fracture Resistance

Figure 13 depicts the delayed fracture test method proposed by Nippon Steel Corporation (NSC)⁽⁷⁾. The test specimens were notched to exhibit a stress concentration factor of 4.6 and immersed in a 5% HCl solution for 30 minutes, and then immediately moved to a constant load test machine to evaluate whether failure occurs or not.

In a 5% HCl acid solution, the reactions are as follows:

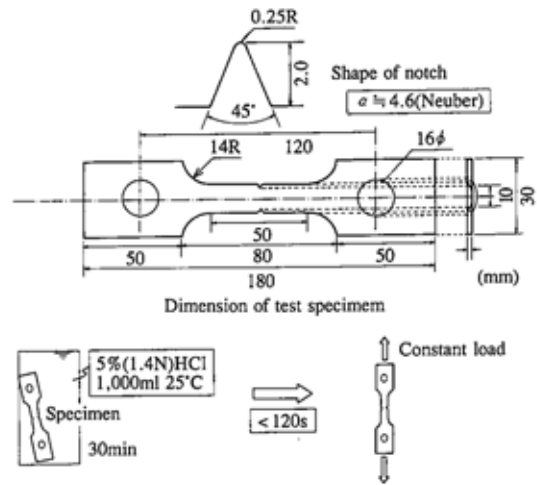
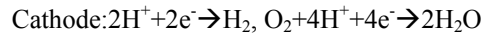
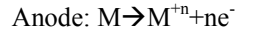


Fig. 13. Schematic illustration of the NSC delayed fracture test⁽⁹⁾.

The constant load test results show that the as-quenched 15B22 steel does not rupture for more than 3 months under the applied loading of yield strength level. This suggests that the as-quenched 15B22 steel exhibits excellent delayed fracture resistance in a dilute HCl solution.

In order to specify the critical allowable hydrogen content of the as-quenched 15B22 steel under the applied loading of yield strength level, specimens were electrochemically charged to various contents of hydrogen and Ni-electroplated to secure the charged hydrogen, and then subjected to a constant load test under the yield strength level. The charged specimens were placed to the cathode in a 0.1N sulfuric acid electrolyte solution under the current density of 10mA/cm². The cathode reaction is $H^+ + e^- \rightarrow H_{\text{adsorption}}$. Furthermore, in order to improve the hydrogen charging effect, trace As₂O₃ was added to inhibit the combination of hydrogen atoms into hydrogen gas.

Figure 14 shows the hydrogen absorption and desorption curves of quenched 15B22 steel by an electrochemical charging and an atmosphere discharging, respectively. It can be found from Fig. 14(a) that the

saturated hydrogen content of 15B22 steel subjected to electrochemical charging for 30 minutes is 4.3 ppm. From Fig. 14(b) it can be found that the absorbed hydrogen atoms will be gradually released in the atmosphere environment at room temperature. After 24 hours, the absorbed hydrogen atoms are almost totally released to fall to the level of 0.68 ppm. This suggests that only very few high binding energy sites exist in the as-quenched 15B22 steel, i.e. most of charged hydrogen atoms are in diffusive status.

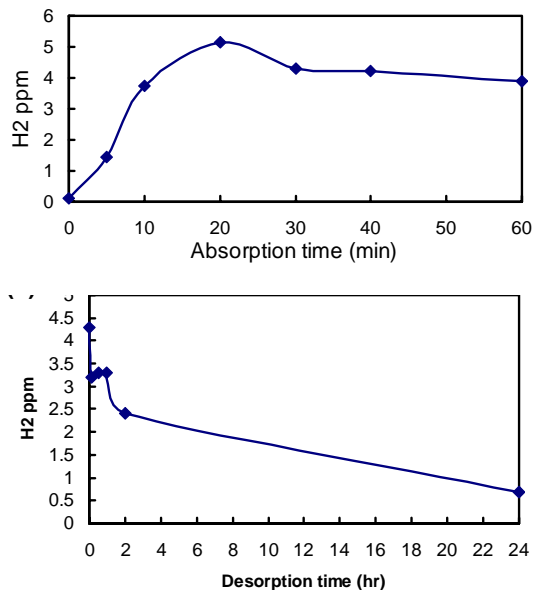


Fig. 14. (a) The hydrogen absorption curve and (b) the hydrogen desorption curve of quenched 15B22 steel by an electrochemical charging and an atmosphere discharging.

To obtain the critical allowable hydrogen content of 15B22 steel, the specimens were electrochemically charged to various contents of hydrogen (1.44 / 2.45 / 3.73 / 4.3 ppm) under the loading of yield strength for 100 hrs. It was found that the specimen with 4.3 ppm charged hydrogen ruptured after yield stress loading, whereas the specimens with charged hydrogen contents lower than 3.73 ppm did not rupture under the same test condition. The fractography of the ruptured specimen with 4.3 ppm charged hydrogen is shown in Figure 15, exhibiting brittle fracture facets. This indicates that the critical allowable hydrogen content of as-quenched 15B22 steel is 3.73 ppm.

4. CONCLUSIONS

(1) The induction quenched 15B22 steel tube for DIB can exhibit an excellent mechanical performance (hardness higher than HV420, TS around 1,600-1,760 MPa, total elongation around 14-16%) which fully satisfies the property requirements of an automobile door impact beam. The predominant microstructure

of hardened 15B22 steel is quenched martensite which is free of carbides inside martensite laths. The prior austenite grain size of as-quenched 15B22 steel, ranging from 2.5 to 8 μm , results in a ductile dimple fractograph after tensile test, indicating an excellent ductility.

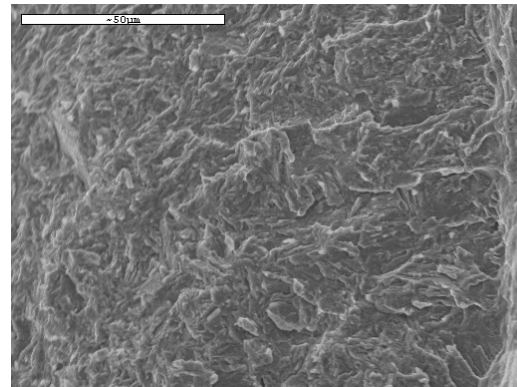


Fig. 15. The fractography of the constant load tested specimen with 4.3 ppm of hydrogen.

(2) The result of the delayed fracture test based on NSC's method shows that the 15B22 steel for impact beam exhibits excellent delayed fracture resistance in a dilute acid environment. By using the electro-chemical charging and the constant load test, the critical allowable hydrogen content for 15B22 steel under the yield strength loading is 3.73 ppm. Experimental results also show that most of the hydrogen trap sites in as-quenched 15B22 steel are low binding energy sites which can not trap the absorbed hydrogen. The impact of application environment must be concerned.

REFERENCES

1. Moto Sato, Yukihiro Utsumi and Kenichi Watanabe, R&D Kobe Steel Engineering Reports, 57(2): 23-26, 2007.
2. Hiroto Tanabe and Kazumasa Yamazaki, United States Patent no. 5181974, Jan. 26, 1993.
3. <http://www.thefabricator.com/>
4. G.E. Totten, G.R. Garsombke, D. Pye and R.W. Reynoldson, Steel Heat Treating Handbook, eds. G.E. Totten and M.A.H. Howes, Marcel Dekker, Inc., New York, NY, 795-800, 1997.
5. Shingo Yamasaki, Manabu Kubota and Toshimi Tarui, Nippon Steel Technical Report, No. 80: 50-55, 1999.
6. J.L.Gu, K.D. Chang, H.S. Fang and B.Z. Bai, ISIJ International, 42(12): 1560-1564, 2002.
7. H. Tanabe, A. Miyasaka, K. Yamazaki, T. Iwasaki and H. Akada, Nippon Steel Technical Report, No.64: 55-61, 1995.